Original Article

Diagnostic Accuracy of 3D Contrast-Enhanced T1 High Resolution Isotropic Volume Excitation MRI for Non-Cavernous Intracranial Dural Arteriovenous Fistula

Theeraphol Panyaping MD[1], Siwipan Changtham MD[1], Patchalin Patputtipong MD[1]

[1] Department of Diagnostic and Therapeutic Radiology, Faculty of Medicine, Ramathibodi Hospital, Mahidol University, Bangkok, Thailand

Objective: To determine the accuracy of 3D contrast-enhanced THRIVE MRI in diagnosis of non-cavernous intracranial dural AVF compared with DSA.

Materials and Methods: Thirty-three patients including fourteen dural AVF cases and nineteen control subjects, were included in the present study. They underwent 3D contrast-enhanced THRIVE MRI by 3T, contrast-enhanced MRA, and DSA. Two independent readers reviewed 3D contrast-enhanced THRIVE images for the presence of transosseous arterial feeders, low signal intensity curvilinear structures in the dural venous sinus, shaggy dural sinus, and cortical venous dilatation. Diagnostic performance values were calculated for 3D contrast-enhanced THRIVE MRI.

Results: The 3D contrast-enhanced THRIVE MRI identified 23 from 29 locations of dural AVFs. The overall accuracy, sensitivity, specificity, positive predictive value, and negative predictive value were 91.4%, 79.3%, 93.5%, 67.6% and 96.3%, respectively. Shaggy dural sinus and dilated cortical veins were found in 78.6% and 85.7%, respectively.

Conclusion: The 3D contrast-enhanced THRIVE MRI is a valuable tool for diagnosis of dural AVF as well as exclusion of dural AVF due to high sensitivity and specificity.

Keywords: Dural arteriovenous fistula; Dural AVF; 3D contrast-enhanced THRIVE MRI

Received 18 November 2019 | Revised 15 October 2021 | Accepted 18 October 2021

J Med Assoc Thai 2021;104(11):1769-76

Website: http://www.jmatonline.com

Intracranial dural arteriovenous fistula (AVF) is a unique vascular malformation that is supplied by dural arteries and drains into dural venous sinuses or meningeal veins[1]. Dural AVFs account for approximately 10% to 15% of intracranial arteriovenous shunts and typically occurred in middle-aged adults with a median age of onset in the sixth decade[2]. They are predominantly idiopathic, though a small percentage of patients have a history of previous craniotomy, trauma, or dural sinus thrombosis[3]. The symptomatology of dural AVF is variable, depending on the location of the shunt, the type of venous drainage, and the flow characteristics[4,5]. Dural AVFs may be asymptomatic, or present with symptoms related to increased dural sinus blood flow, such as pulsatile tinnitus, which is particularly common for transverse and sigmoid sinuses lesions[4,6,7].

Digital subtraction angiography (DSA) remains the gold standard for detection of intracranial dural AVF[8]. However, the relatively invasive nature of angiography limits its application as a rule-in study[9]. Computed tomography angiography (CTA) and magnetic resonance angiography (MRA) may detect the fistula and can be used to screen the patients with clinical suspicion of dural AVF[2]. The characteristic findings of dural AVF on CTA and MRA include enlarged feeding arteries, early dural sinus opacification, and prominent draining veins[10-12]. However, these characteristic findings of dural AVF were incidentally found on 3D contrast-enhanced T1 high resolution isotropic volume excitation (THRIVE) magnetic resonance imaging (MRI) in some patients without clinical suspicion of dural AVF.

The 3D THRIVE MRI is 3D ultrafast spoiled gradient echo with isotropic data acquisition that does not show partial volume averaging artifacts providing more anatomical detail and pathological information of small complex areas. Contrast-enhanced THRIVE MRI shows good contrast opacification in the cerebral

Correspondence to:

Patputtipong P.

Department of Diagnostic and Therapeutic Radiology, Faculty of Medicine, Ramathibodi Hospital, Mahidol University, Bangkok 10400, Thailand.

Phone: +66-2-2011000, **Fax**: +66-2-2011297

Email: mdpatchalin@gmail.com

How to cite this article:

Panyaping T, Changtham S, Patputtipong P. Diagnostic Accuracy of 3D Contrast-Enhanced T1 High Resolution Isotropic Volume Excitation MRI for Non-Cavernous Intracranial Dural Arteriovenous Fistula. J Med Assoc Thai 2021;104:1769-76.

doi.org/10.35755/jmedassocthai.2021.11.10870

venous structures and even in cerebral arteries with minimized flow-related artifacts[13]. The application of 3D ultrafast spoiled gradient echo improves the dynamic liver, gastrointestinal tract, breast, prostate, and brain imaging studies[14-18].

Prior studies found that 3D contrast-enhanced ultrafast spoiled gradient echo with magnetization preparation (MP-RAGE) could depict the venous anomaly and cerebral venous disease[19,20]. To the authors' knowledge, no study of 3D contrast-enhanced THRIVE MRI in diagnosis of intracranial dural AVF has been found in the literature.

The purpose of the present study was to determine accuracy of 3D contrast-enhanced THRIVE in diagnosis of non-cavernous intracranial dural AVF compared with DSA.

Materials and Methods

Study setting

The present study was conducted in the Department of Diagnostic and Therapeutic Radiology of the Ramathibodi Hospital. The study was approved by the Institutional Ethics Committee (COA MURA2016/206/NP). The informed consent was waived.

Patient selection

The cross-sectional study of non-cavernous intracranial dural AVF patients that underwent 3D contrast-enhanced THRIVE MRI, contrast-enhanced MRA, and DSA between January 2011 and December 2016, were searched on the hospital imaging information system. The inclusion criteria were the subjects older than 15 years old with diagnosis of non-cavernous intracranial dural AVF from DSA and that underwent pretreatment 3D contrast-enhanced THRIVE MRI. The exclusion criteria were incomplete or poor quality MRI examination, and status post treatment.

A similar search on the authors' hospital image information system was performed to identify the control group. They had performed 3D contrast-enhanced THRIVE MRI, contrast-enhanced MRA and DSA due to clinical suspicion of dural AVF, pulsatile tinnitus, or headache. They were not diagnosed as dural AVF or dural venous sinus abnormality by DSA or contrast-enhanced MRA with no clinical concern about dural AVF on interval clinical follow up.

3D contrast-enhanced THRIVE technique

The MRI examination was performed at 3.0T (Philips Intera, Philips Medical Systems, Best, Netherland scanners) with a 32-channel head coil. Routine conventional MRI with 3D contrast-enhanced THRIVE were performed. Intravenous contrast material of 0.1 mmol/kg was administered by hand injection, then THRIVE sequence was obtained at 6 to 10 minutes after injection time. The 3D contrast-enhanced THRIVE sequence was applied with the following parameters: TR/TE=6/3 ms, a flip angle of 12°, 0.5 mm slice thickness, a FOV of 24 cm, a matrix of 240×240 and an acquisition time of two to four minutes. This sequence was oriented in the axial plane with coronal and sagittal reconstructions.

DSA

The DSA was performed on a flat panel biplane system. The study included both internal and external carotid arteries and vertebral arteries with at least two intracranial views, which were AP and lateral views. Each angiogram was acquired at three frames per second with 1048×1048 matrix size and 12-inch FOV.

MRI analysis

Two neuroradiologists including one with six and one with three years of experience in brain MRI were blinded to the patient information and final diagnosis. Both neuroradiologists independently reviewed 3D contrast-enhanced THRIVE images to document the following findings 1) feeding arteries defined as transosseous enhancing curvilinear structures connecting to the dural sinus wall, and 2) low signal intensity curvilinear structures within dural sinus (Figure 1, 2). The diagnosis of DAVF was made in case with 1) plus 2) findings. The location of fistula was identified as superior sagittal dural sinus, torcular herophili, right and left transverse dural sinus, right and left sigmoid dural sinus. Shaggy dural sinus wall and cortical vein dilatation were the additional imaging findings.

The readers were blinded to the clinical history, imaging results, and diagnosis. Any discrepancy in the interpretation was resolved by consensus.

Five pilot case studies took place prior to the full study to ensure that the two readers were consistent on the definition of imaging features.

Statistical analysis

All statistical analyses were programmed in IBM SPSS Statistics, version 24 (IBM Corp., Armonk, NY, USA). Comparisons on continuous variables among the groups were performed by using unpaired t-test and Mann-Whitney U test. Chi-squared test or Fisher's exact test was used to test categorical

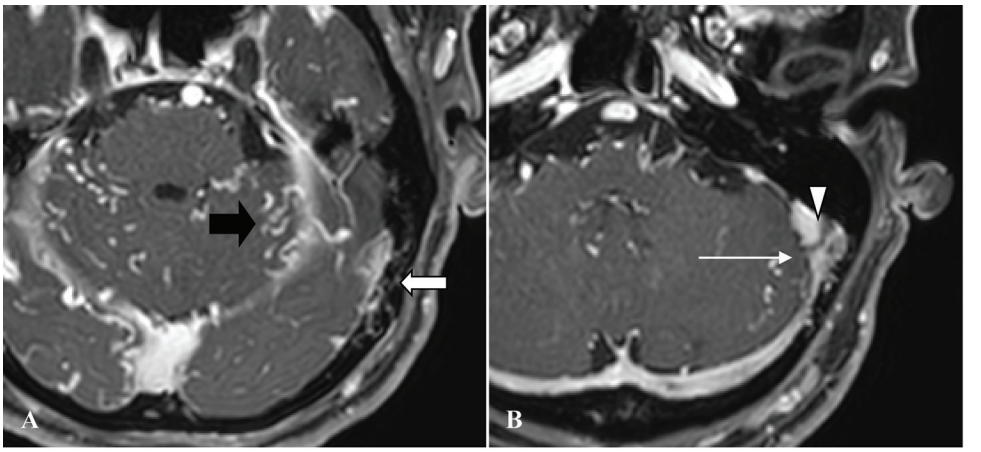

Figure 1. Dural AVF at the left sigmoid sinus. (A, B) Axial 3D contrast-enhanced THRIVE MRI shows transosseous enhancing curvilinear structures adjadent to dural venous sinus wall (thick white arrow), consistent with transosseous feeding arteries. There are low intensity curvilinear structures within dural venous sinus (arrow head). Shaggy sinus at left sigmoid sinus (thin white arrow) and cortical venous dilatation (black arrow) is also observed.

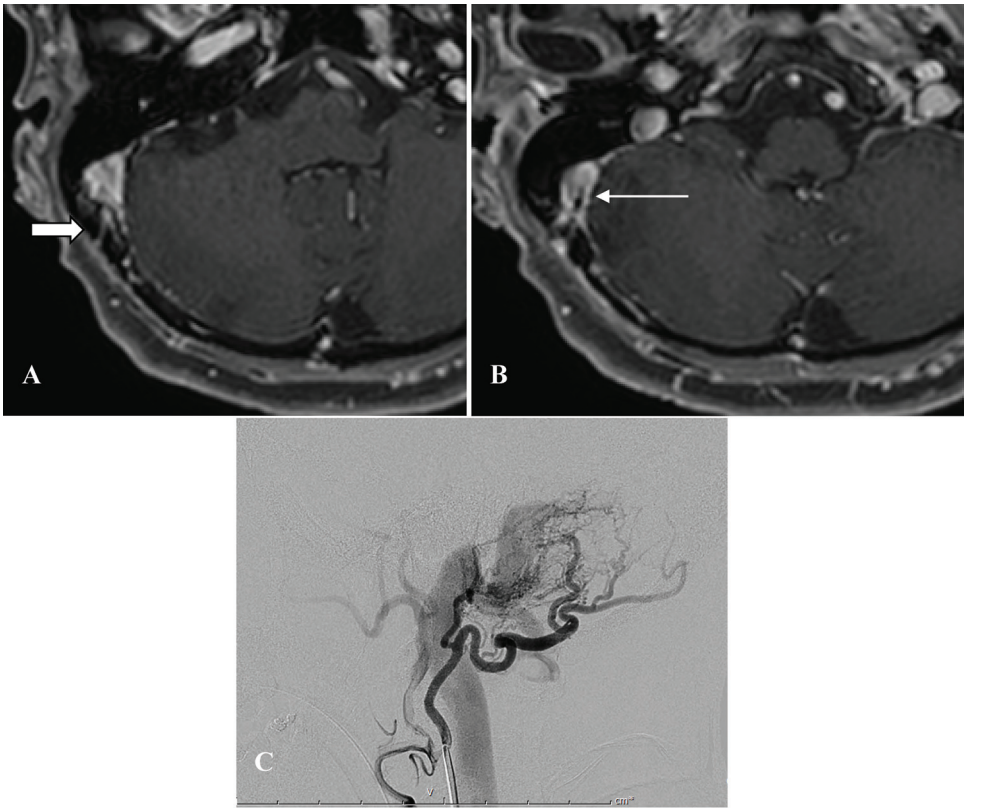

Figure 2. Dural AVF at the right sigmoid sinus. (A, B) Axial 3D contrast-enhanced THRIVE MRI shows transosseous feeding arteries (thick white arrow), low intensity curvilinear structures in dural sinus (thin white arrow) and shaggy sinus at the right sigmoid sinus. (C) DSA reveals benign dural AVF at the right sigmoid sinus.

variables. Fisher's exact test was used once numbers were small. A p-value of less than 0.05 was considered a statistically significant difference. The accuracy, sensitivity, specificity, positive predictive value, negative predictive value and 95% confidence interval (CI) were analyzed. Agreement between the two

Table 1. Demographic data

Demographic data	Control (n=19)	Case (n=14)	p-value
Age (years); mean±SD	51.79±15.0	61.21±12.5	0.065
Sex; n (%)			0.003
Male	4 (21.1)	10 (71.4)	
Female	15 (78.9)	4 (28.6)	

SD=standard deviation

Table 2. Identification of dural AVF on DSA

Location	n (%)
Transverse sinus (right + left)	11 (37.9)
Sigmoid sinus (right + left)	8 (27.6)
Torcular herophili	7 (24.1)
Superior sagittal sinus	3 (10.4)
Total	29 (100)

AVF=arteriovenous fistula; DSA=digital subtraction angiography; SSS=superior sagittal sinus

Table 3. Sensitivity, specificity, PPV, and NPV of 3D contrast-enhanced THRIVE MRI in diagnosis of dural AVF

Location	Sensitivity (95% CI)	Specificity (95% CI)	PPV (95% CI)	NPV (95% CI)
Sigmoid sinus	87.5% (46.6 to 99.3)	98.3% (89.8 to 99.9)	87.5% (46.6 to 99.3)	98.3% (89.8 to 99.9)
Transverse sinus	81.8% (47.7 to 96.7)	85.5% (56.1 to 97.4)	52.9% (47.7 to 96.7)	95.9% (56.1 to 97.4)
Torcular herophili	71.4% (30.2 to 94.8)	90.2% (57.1 to 99.5)	83.3% (36.4 to 99.1)	92.6% (50.8 to 97.0)
SSS	66.7% (12.5 to 98.2)	96.7% (80.9 to 99.8)	66.7% (12.5 to 98.2)	96.7% (80.9 to 99.8)
Overall	79.3% (59.7 to 91.2)	93.5% (88.4 to 96.5%)	67.6% (49.3 to 82.0)	96.3% (91.9 to 98.5)

PPV=positive predictive value; NPV=negative predictive value; CI=confidence interval; SSS=superior sagittal sinus

readers was evaluated by the use of the weighted κ statistic. A kappa value of 0.81 to 1.0 was considered as excellent agreement, 0.61 to 0.80 good agreement, 0.41 to 0.6 moderate agreement, 0.21 to 0.4 fair agreement, and 0 to 0.2 slight agreement[21,22].

Results

Thirty-three patients were included in the present study (Table 1). There were 14 (42.4%) patients of dural AVF and 19 (57.6%) patients of control group. The 2-tailed independent-samples t-test demonstrated that there was no significant difference in mean age with the case at 61.2 years and the control at 51.8 years (p=0.065) between the two groups. Significant difference in gender predominance between groups was identified. Control group was female predominated, while case group was male predominated.

In the control group, DSA was performed in one patient. The remaining cases had normal contrast-enhanced MRA with no clinical concern about dural AVF on interval clinical follow up.

In patients with dural AVF, 29 fistula sites were identified by DSA. The transverse dural sinus was the most common fistula site with 11 fistula sites (37.9%). The fistula sites at the sigmoid, torcular herophili, and superior sagittal sinus were eight (27.6%), seven (24.1%), and three (10.4%), respectively (Table 2).

Table 4. False positive and false negative cases in diagnosis of dural AVF

Location	False positive (No.)	False negative (No.)
Transverse sinus	8	2
Sigmoid sinus	1	1
Torcular herophili	1	2
SSS	1	1
Total	11	6

SSS=superior sagittal sinus

The 3D contrast-enhanced THRIVE MRI identified 23 from 29 locations of dural AVFs. On 3D contrast-enhanced THRIVE MRI, the overall accuracy, sensitivity, specificity, positive predictive value, and negative predictive value of diagnosis of dural AVF were 91.4%, 79.3%, 93.5%, 67.6%, and 96.3%, respectively (95% CI 60.3 to 92.0). The accuracy, sensitivity, specificity, positive predictive value, and negative predictive value of each location are listed in Table 3. The shaggy sinus and cortical venous dilatation were identified in 11 cases (78.6%) and 12 cases (85.7%), respectively. The false positive and false negative cases are listed in Table 4. Most false positive cases, in eight of eleven patients, were found at the transverse sinus (Figure 3), whereas, most false negative cases were found at the transverse sinus in two of six patients and

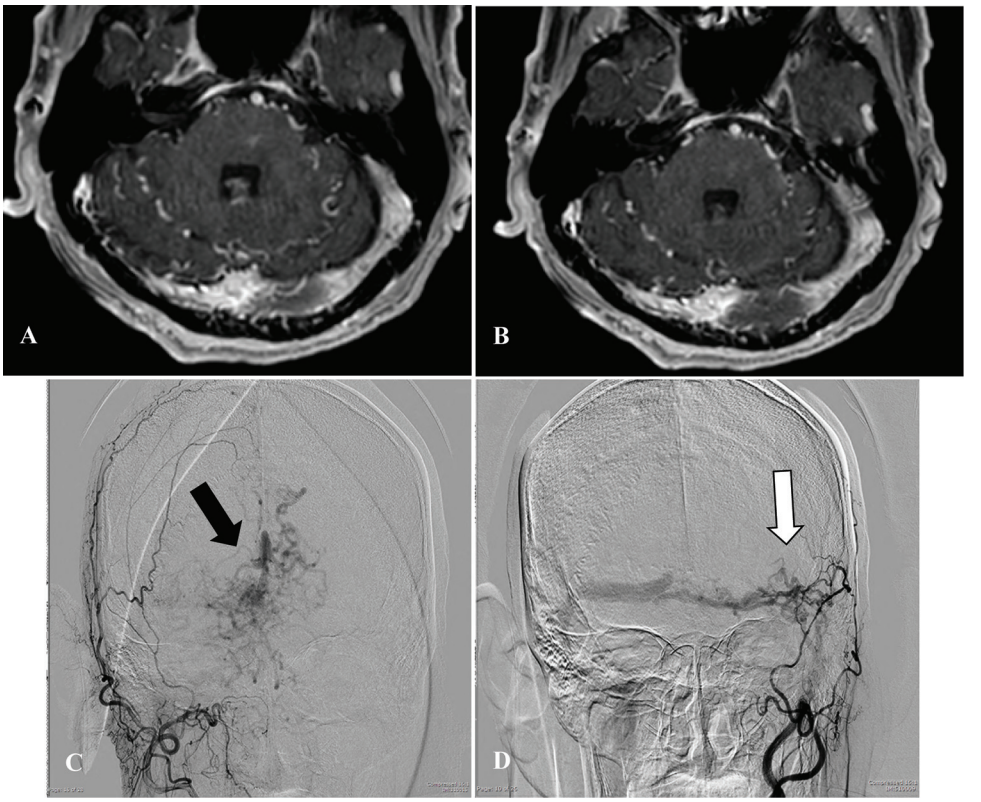

Figure 3. Dural AVF at the torcular herophili and left transverse sinus. (A, B) Axial 3D contrast-enhanced THRIVE MRI reveals transosseous feeding arteries and low intensity curvilinear structures in bilateral transverse sinuses and torcular herophili, suggestive of dural AVF at the bilateral transverse sinuses and torcular herophili. (C, D) DSA reveals dural AVF at the left transverse sinus (white arrow) and torcular herophili (black arrow). No dural AVF is found at the right transverse sinus on DSA.

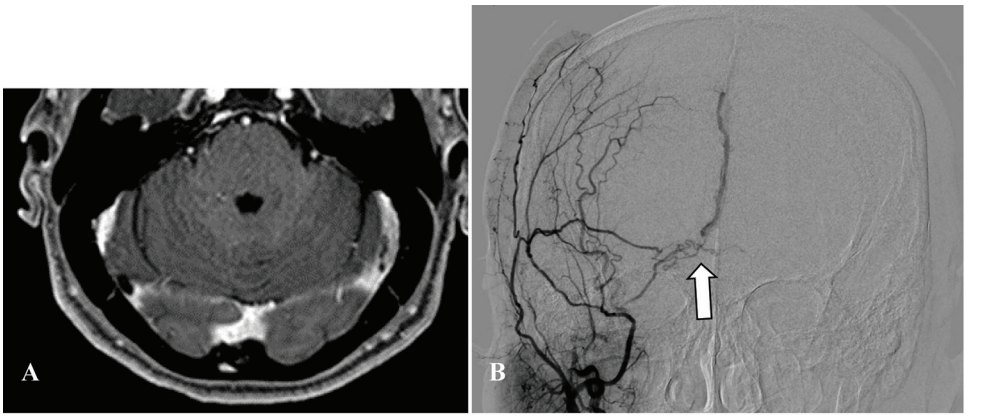

Figure 4. Dural AVF at the torcular herophili. (A) Axial 3D contrast-enhanced THRIVE MRI shows no evidence of dural AVF. (B) DSA reveals small dural AVF at the torcular herophili (arrow), which is fed by petrosquamosal branch of the right middle meningeal artery.

torcular herophili in two of six patients (Figure 4). The mean duration gap between 3D contrast-enhanced THRIVE and DSA was 13.6 days with a range of 1 to 52 days.

The k test revealed moderate to excellent level of interobserver agreement in the reading with k=0.446 to 0.864.

Discussion

Conventional MRI may be the initial imaging

study in patients with dural AVF due to variable clinical presentations. Flow void in dural venous sinus and fistula site on conventional MRI were used to diagnose dural AVF with low sensitivity and specificity. Jain et al demonstrated flow void and probable location of fistula in only 46% and 19% of patients of dural AVF, respectively[23]. Furthermore, normal conventional MRI does not exclude the presence of dural AVF.

The SWI image was recognized for diagnosis of dural AVF with advantage of non-contrast enhanced study. Tsui et al, demonstrated hyperintensities within the draining venous sac or sinuses due to rapid shunting of blood with oxyhemoglobin[24]. Letourneau-Guillon and Krings observed hyperintense venous structures on SWI as possible location of the fistula in five of six patients[25]. In agreement with the study of Jain et al that found SWI accurately located 75% of all fistula sites in 23 patients[23].

The present study demonstrated a role of 3D contrast-enhanced THRIVE MRI in diagnosis of dural AVF with high accuracy (91.4%) and specificity (93.5%). In patients with dural AVF, transosseous enhancing curvilinear structures adjacent to dural venous sinus wall and low intensity curvilinear structures within dural venous sinus were depicted on 3D contrast-enhanced THRIVE MRI. The finding of transosseous enhancing curvilinear structures adjacent to dural venous sinus wall likely represents transosseous feeding arteries of the dural AVF at the fistula site. The low intensity curvilinear structures within the dural venous sinus may represent flow-related venous artifacts due to high flow velocity or arterialization of venous sinus rather than crack-like vessels secondary to angiogenesis within dural sinus[26].

Two most common locations of dural AVF in the present study were at transverse and sigmoid sinuses similar to the previous reports[27,28]. In the present study, 3D contrast-enhanced THRIVE MRI demonstrated highest sensitivity and specificity in these locations with 81.8%/87.5%, and 85.5%/98.3%, respectively. High negative predictive value of 96.3% of 3D contrast-enhanced THRIVE MRI was observed. As a result, the physicians may be able to use 3D contrast-enhanced THRIVE MRI for diagnostic exclusion of dural AVF.

The present study found shaggy sinus and cortical venous dilatation in most cases. Narvid et al observed shaggy sinus on CTA and found in four out of seven patients with dural AVF and pulsatile tinnitus[10]. This finding represents a conglomeration of pathologic sequelae implicated in the angiogenic process.

Cortical venous dilatation suggests presence of venous congestion, which is aggressive feature of dural AVF in both Borden and Cognard classifications[29,30]. Willinsky et al reviewed pseudophlebitic pattern or engorged veins in 130 patients with intracranial dural AVF and this finding was found in 51 patients (42%)[31]. The pathogenetic mechanism of the cortical vein dilatation was explained by the involved dural venous sinus receiving arterialized blood flow that can lead to mechanical obstruction of the sinus and result in retrograde drainage of blood into the cortical veins[32]. This aggressive feature indicates malignant dural AVF, which correlates with an increased likelihood of intracerebral hemorrhage and aggressive symptoms[33]. In the present study, 12 of 14 cases were malignant dural AVF resulting in high incidence of cortical venous dilatation.

Almost all false positive cases were found at the transverse sinus. This may correspond to major dural venous variations identified in the transverse and sigmoid sinuses, such as septation or normal transosseous vessels[34]. Adjacent dural AVF can interfere with interpretation of transosseous feeding arteries. Long duration gap between 3D contrast-enhanced THRIVE MRI and DSA may cause changes of the disease such as shunt location or size of shunt. Six false negative cases were noted, most of them had small shunt.

The interobserver agreement revealed moderate to excellent levels. The detection of fistula at the right transverse sinus shows highest interobserver agreement, which may be due to relatively large size of the right transverse sinus compared with that of the left side[35].

However, the present study had some limitations. First, this was a crossectional study with small sample size. Second, malignant type of dural AVF was the type that may increase sensitivity and specificity of the study. Third, DSA was performed in only one patient of the control group. The remaining cases of the control group were not performed DSA due to evidence of normal contrast-enhanced MRA and no clinical concern about dural AVF on interval clinical follow up. Fourth, duration gap between 3D contrast-enhanced THRIVE MRI and DSA in the present study ranged between one day and two months and spontaneous change of the dural AVF may occur and cause changes of the imaging findings.

Conclusion

The 3D contrast-enhanced THRIVE is a valuable

tool for diagnosis of dural AVF. It also provides the information for exclusion of dural AVF.

What is already known on this topic?

There have been many previous studies using conventional MRI, SWI sequence, and MRA in diagnosis of dural AVF. This study represents the first study to determine diagnostic accuracy of 3D contrast-enhanced THRIVE MRI in diagnosis of intracranial dural AVF compared with DSA.

What this study adds

The 3D contrast-enhanced THRIVE MRI is an MRI technique that well demonstrate intracranial venous structures with high accuracy, sensitivity, and specificity in diagnosis of dural AVF.

Conflicts of interest

The authors declare no conflict of interest.

References

1. Kwon BJ, Han MH, Kang HS, Chang KH. MR imaging findings of intracranial dural arteriovenous fistulas: relations with venous drainage patterns. AJNR Am J Neuroradiol 2005;26:2500-7.
2. Serulle Y, Miller TR, Gandhi D. Dural arteriovenous fistulae: Imaging and management. Neuroimaging Clin N Am 2016;26:247-58.
3. Gandhi D, Chen J, Pearl M, Huang J, Gemmete JJ, Kathuria S. Intracranial dural arteriovenous fistulas: classification, imaging findings, and treatment. AJNR Am J Neuroradiol 2012;33:1007-13.
4. Miller TR, Gandhi D. Intracranial dural arteriovenous fistulae: Clinical presentation and management strategies. Stroke 2015;46:2017-25.
5. Sarma D, ter Brugge K. Management of intracranial dural arteriovenous shunts in adults. Eur J Radiol 2003;46:206-20.
6. Kim MS, Han DH, Kwon OK, Oh CW, Han MH. Clinical characteristics of dural arteriovenous fistula. J Clin Neurosci 2002;9:147-55.
7. Saito A, Takahashi N, Furuno Y, Kamiyama H, Nishimura S, Midorikawa H, et al. Multiple isolated sinus dural arteriovenous fistulas associated with antithrombin III deficiency--case report. Neurol Med Chir (Tokyo) 2008;48:455-9.
8. Wetzel SG, Bilecen D, Lyrer P, Bongartz G, Seifritz E, Radue EW, et al. Cerebral dural arteriovenous fistulas: detection by dynamic MR projection angiography. AJR Am J Roentgenol 2000;174:1293-5.
9. Lin YH, Lin HH, Liu HM, Lee CW, Chen YF. Diagnostic performance of CT and MRI on the detection of symptomatic intracranial dural arteriovenous fistula: a meta-analysis with indirect comparison. Neuroradiology 2016;58:753-63.
10. Narvid J, Do HM, Blevins NH, Fischbein NJ. CT angiography as a screening tool for dural arteriovenous fistula in patients with pulsatile tinnitus: feasibility and test characteristics. AJNR Am J Neuroradiol 2011;32:446-53.
11. Noguchi K, Melhem ER, Kanazawa T, Kubo M, Kuwayama N, Seto H. Intracranial dural arteriovenous fistulas: evaluation with combined 3D time-of-flight MR angiography and MR digital subtraction angiography. AJR Am J Roentgenol 2004;182:183-90.
12. Chen JC, Tsuruda JS, Halbach VV. Suspected dural arteriovenous fistula: results with screening MR angiography in seven patients. Radiology 1992;183:265-71.
13. Ahn SS, Kim J, An C, Choi HS, Lee SK, Koh YW, et al. Preoperative imaging evaluation of head and neck cancer: comparison of 2D spin-echo and 3D THRIVE MRI techniques with resected tumours. Clin Radiol 2012;67:e98-104.
14. Martin DR, Danrad R, Herrmann K, Semelka RC, Hussain SM. Magnetic resonance imaging of the gastrointestinal tract. Top Magn Reson Imaging 2005;16:77-98.
15. Mohindra N, Neyaz Z. Magnetic resonance sequences: Practical neurological applications. Neurol India 2015;63:241-9.
16. Hegde JV, Mulkern RV, Panych LP, Fennessy FM, Fedorov A, Maier SE, et al. Multiparametric MRI of prostate cancer: an update on state-of-the-art techniques and their performance in detecting and localizing prostate cancer. J Magn Reson Imaging 2013;37:1035-54.
17. Coenegrachts K, Ghekiere J, Denolin V, Gabriele B, Hérigault G, Haspeslagh M, et al. Perfusion maps of the whole liver based on high temporal and spatial resolution contrast-enhanced MRI (4D THRIVE): feasibility and initial results in focal liver lesions. Eur J Radiol 2010;74:529-35.
18. Thomassin-Naggara I, Trop I, Lalonde L, David J, Péloquin L, Chopier J. Tips and techniques in breast MRI. Diagn Interv Imaging 2012;93:828-39.
19. Liang L, Korogi Y, Sugahara T, Onomichi M, Shigematsu Y, Yang D, et al. Evaluation of the intracranial dural sinuses with a 3D contrast-enhanced MP-RAGE sequence: prospective comparison with 2D-TOF MR venography and digital subtraction angiography. AJNR Am J Neuroradiol 2001;22:481-92.
20. Liang L, Korogi Y, Sugahara T, Ikushima I, Shigematsu Y, Takahashi M, et al. Normal structures in the intracranial dural sinuses: delineation with 3D contrast-enhanced magnetization prepared rapid acquisition gradient-echo imaging sequence. AJNR Am J Neuroradiol 2002;23:1739-46.
21. Fleiss JL, Levin B, Paik MC. The measurement of interrater agreement. In: Fleiss JL, Levin B, Paik MC, editors. Statistical Methods for Rates and Proportions. 3rd ed. Hoboken, NJ: John Wiley & Sons; 2004. p.

598-626.
22. Landis JR, Koch GG. The measurement of observer agreement for categorical data. Biometrics 1977;33:159-74.
23. Jain NK, Kannath SK, Kapilamoorthy TR, Thomas B. The application of susceptibility-weighted MRI in pre-interventional evaluation of intracranial dural arteriovenous fistulas. J Neurointerv Surg 2017;9:502-7.
24. Tsui YK, Tsai FY, Hasso AN, Greensite F, Nguyen BV. Susceptibility-weighted imaging for differential diagnosis of cerebral vascular pathology: a pictorial review. J Neurol Sci 2009;287:7-16.
25. Letourneau-Guillon L, Krings T. Simultaneous arteriovenous shunting and venous congestion identification in dural arteriovenous fistulas using susceptibility-weighted imaging: initial experience. AJNR Am J Neuroradiol 2012;33:301-7.
26. Hamada Y, Goto K, Inoue T, Iwaki T, Matsuno H, Suzuki S, et al. Histopathological aspects of dural arteriovenous fistulas in the transverse-sigmoid sinus region in nine patients. Neurosurgery 1997;40:452-6.
27. Fermand M, Reizine D, Melki JP, Riche MC, Merland JJ. Long term follow-up of 43 pure dural arteriovenous fistulae (AVF) of the lateral sinus. Neuroradiology 1987;29:348-53.
28. Levrier O, Métellus P, Fuentes S, Manera L, Dufour H, Donnet A, et al. Use of a self-expanding stent with balloon angioplasty in the treatment of dural arteriovenous fistulas involving the transverse and/or sigmoid sinus: functional and neuroimaging-based outcome in 10 patients. J Neurosurg 2006;104:254-63.
29. Cognard C, Gobin YP, Pierot L, Bailly AL, Houdart E, Casasco A, et al. Cerebral dural arteriovenous fistulas: clinical and angiographic correlation with a revised classification of venous drainage. Radiology 1995;194:671-80.
30. Borden JA, Wu JK, Shucart WA. A proposed classification for spinal and cranial dural arteriovenous fistulous malformations and implications for treatment. J Neurosurg 1995;82:166-79.
31. Willinsky R, Goyal M, terBrugge K, Montanera W. Tortuous, engorged pial veins in intracranial dural arteriovenous fistulas: correlations with presentation, location, and MR findings in 122 patients. AJNR Am J Neuroradiol 1999;20:1031-6.
32. Signorelli F, Della Pepa GM, Sabatino G, Marchese E, Maira G, Puca A, et al. Diagnosis and management of dural arteriovenous fistulas: a 10 years single-center experience. Clin Neurol Neurosurg 2015;128:123-9.
33. Rahman WT, Griauzde J, Chaudhary N, Pandey AS, Gemmete JJ, Chong ST. Neurovascular emergencies: imaging diagnosis and neurointerventional treatment. Emerg Radiol 2017;24:183-93.
34. McCormick MW, Bartels HG, Rodriguez A, Johnson JE, Janjua RM. Anatomical variations of the transverse-sigmoid sinus junction: Implications for endovascular treatment of idiopathic intracranial hypertension. Anat Rec (Hoboken) 2016;299:1037-42.
35. Leach JL, Fortuna RB, Jones BV, Gaskill-Shipley MF. Imaging of cerebral venous thrombosis: current techniques, spectrum of findings, and diagnostic pitfalls. Radiographics 2006;26 Suppl 1:S19-41; discussion S2-3.